UNIZIK JOURNAL OF ENGINEERING AND APPLIED SCIENCES (UJEAS)

Research Article

Particle Size Variation on the Characteristics of Pretreated APWF-LLDPE Composite for Furniture Component of Automobile Parts Production

Government R. M., Ayuba S.

Special Issue
A Themed Issue in Honour of Professor Clement Uche Atuanya on His retirement.

This themed issue pays tribute to Professor Clement Uche Atuanya in recognition of his illustrious career in Metallurgical and Materials Engineering as he retires from Nnamdi Azikiwe University, Awka. We celebrate his enduring legacy of dedication to advancing knowledge and his impact on academia and beyond through this collection of writings.

Edited by
Chinonso Hubert Achebe PhD.
Christian Emeka Okafor PhD.

UJEAS

UNIZIK JOURNAL OF ENGINEERING AND APPLIED SCIENCES

UNIZIK Journal of Engineering and Applied Sciences 3(3), September (2024), 846-860
Journal homepage: https://journals.unizik.edu.ng/index.php/ujeas
PRINT ISSN: 2992-4383 || ONLINE ISSN: 2992-4391

Particle Size Variation on the Characteristics of Pretreated APWF-LLDPE Composite for Furniture Component of Automobile Parts Production

Government R. M.[1*] and Ayuba S.[2]
[1] Department of Chemical Engineering, Federal University Wukari, Taraba State, Nigeria
[2] Department of Agricultural Engineering, Federal University Wukari, Taraba State, Nigeria
[*]Corresponding Author's E-mail: govt_4real@yahoo.com

Abstract
The study examined the variation of particles on the characteristics of avocado pear wood fiber-linear-low-density polyethylene (APWF-LLDPE) composite by several treatment rout. The avacodo wood (APWF) with sizes of 150, 180, 250, 425 and 850 µm was compounded in the linear –low-density polyethylene (LLDPE) matrix. The APWF with content ranges from 5-25 wt.% for the variant particle sizes were treated with NaOH (NST), NaOH/CH_3COOH (AAT), NaOH/ CH_3COOH/MAPE (MPT); and blended with LLDPE to form APWF-LLDPE composite, respectively. The manufactured composites made by blending of APWF and LLDPE were passed through mechanical, water absorptive, FTIR and SEM testing, The observable outcome indicated that the characteristics and the resistance to sorption capacity of APWF-LLDPE composite enhanced at 150 µm particle of APWF. The greatest properties of APWF-LLDPE composite was obtained after compounding the APWF modified with NaOH/CH_3COOH/MAPE at the minimum size range and LLDPE matrix. The ultimate strength, modulus of elasticity, bending strength, bending modulus, Brinell hardness, impact energy per unit area and sorption resistance at this particle and 25 wt.% content were equivalent to 24.85 MPa, 0.871 GPa, 63.11 MPa, 0.821 GPa, 788 Pa, 90.35 KJ/m^2 and 3.49 %, respectively. The APWF-LLDPE composite chemically modified NaOH/CH_3COOH/MAPE is a suitable alternative for furniture panel of automotive parts.

Keywords: APWF, LLDPE, APWF-LLDPE composite, particle size, pre-treatment, mechanical characteristics

1. Introduction

Wood fiber is one of the biomass that has many merits in the application of finished products such as automobile and furniture purposes from polymer composite(Azeez et al., 2018; Azeez et al., 2019; Azeez et al., 2021; Ng et al., 2010; Dungani et al., 2016; Obasi, 2015; Fortunati et al., 2019; Government et al., 2018(a-b); Government et al., 2019 (a-c)). These include less energy usage due to low-mass per volume, cost reduction and easily accessibility of raw material, etc. (Catto & Santana, 2018; Government et al., 2019 (a-d); Obasi, 2015). Notwithstanding, this is the reason, it is usually recommends over mineral fiber in composite production. This fiber is a major additive as a component of polymer composite (Government et al., 2018(a-b); Government et al., 2019 (a-c)). Globally, the utilization has spread all over the spectrum of structural artifact in human activities (Government et al., 2018(a-b); Government et al., 2019 (a-c)). Enormous woody species situate in African due to nature of vegetation in which Nigerian is one the country surrounds with large vegetation(Government et al., 2018(a-b); Government et al., 2019 (a-c); Orji &MacDonald, 2020; Rashid et al., 2016)-

The avocado pear wood fiber (APWF) is one of the timbers in which the habitant in the country concentrates in engulfing the fruits from the tree with less awareness in applying it as a component in composite material (Government et al., 2018(a-b); Government et al., 2019 (a-c); Government & Okeke, 2024). Therefore, the APWF has enormous cellulosic components which are the essential constituent in composite material that displays vital characteristics of the products. Few studies has testified that the APWF when filled in polymeric material produces polymer composite that can be interfaced properly whose properties is higher than the fiber or the matrix (Government, 2018(a-b); Government et al., 2019 (a-c); Government & Okeke, 2024).

Furthermore, the APWF improves the structural, mechanical, electrical, heat resistance and dimensional characteristic of the APWF/polymer composite (Government, 2018(a-b); Government et al., 2019 (a-c)). The strength of APWF is a dependency on the nature and the age of the plant. Therefore, those woody fibers that have longer age has the tendency to exhibit huge cellulosic content (Government et al., 2019 (a-d); Obasi, 2015; Government & Okeke, 2024)). In the same vein, they also have the ability to demonstrate the required strength which is enough to maximize the micro-mechanical properties of the composite. As stated from earlier works, the fiber with lofty cellulosic components stands the chances of recording utmost mechanical strength (Fortunati et al., 2019; Government and Ngabea, 2023(a, b)).

The mechanical properties of APWF in polymer matrix composite are the products of these variables: fiber content and size, pretreatment parameters, nature of modifying and bonding reagent, polymer, temperature of production, processing rout used, etc. (Patpen et al, 2015; Government, 2021(a); Kandar & Akil, 2016; Government et al., 2022; Homkhiew et al., 2014; Government et al, 2019(a-d); Peng et al., 2015; Rostamiyan et al., 2015). Moreover, it is advisable for examination of numerous constraints to manufacture APWF/polymer matrix composite with exceptional characteristics (Government et al., 2022). Particle size and fiber content of APWF filled is another determinant on the characteristics of APWF/polymer matrix (Government et al., 2022; Laadila et al., 2017; Turku et al., 2018). This depends on the type of polymer introduced or treated fiber infuses in the polymer matrix. Though, the polymer matrix with huge density returns higher strength to be applicable for heavier structural materials Chanda, 2015; Government et al., 2022; Homkhiew, Rostamiyan et al., 2014(a); Laadila et al., 2017; Zakaria et al., 2018)). In the reverse situation, lower denser polymers are applicable to lower structural engineering materials (Government & Ngebea, 2023 (a, b); Government & Okeke, 2023; Government & Okeke, 2024). Also, processing rout is a constraint which determines the nature of polymer and type of fiber to be involved in the production of APWF/polymer(Patpen et al, 2015; Government, 2021(a); Kandar & Akil, 2016; Government et al., 2022; Homkhiew et al., 2014; Government et al,, 2019(a-d); Peng et al., 2015; Rostamiyan et al., 2015).

The injection molding normally applied for low density polymer and when the fiber is in particulate, while resin transfer molding and hand-layup process are frequently applicable for long fiber and high-density polymers Government & Ngebea, 2023a, b; Government & Okeke, 2023; Government & Okeke, 2024). Extrusion yields good composite due to processing steps that lead to the final products (Government & Ngebea, 2023 (a, b); Government & Okeke, 2023; Government & Okeke, 2024). Temperature impacts more effect of the properties of APWF/polymer composite Government & Ngebea, 2023 (a, b); Government & Okeke, 2023; Government & Okeke, 2024). The APWF/polymer composite establishes above the optimum temperature results to lower micro-mechanical properties (Government & Ngebea, 2023 (a, b); Government & Okeke, 2023; Government & Okeke, 2024). The ultimate operating temperature ensures higher characteristic of the composites (Government & Ngebea, 2023 (a, b); Government & Okeke, 2023; Government & Okeke, 2024).

Pretreatment is paramount for the fiber to relinquish superlative properties in the polymer matrix composite (Aimi et al, 2014; Rashid et al., 2016). Mainly, when the fiber undergoes the stages of treatment minimizes non-conducive constituents (Atuanya et al., 2014; Government et al., 2019(b)). These non-conducive components in the APWF reduces the conjunction of APWF and polymer matrix, incapacitated stress transfer, minimal mechanical properties and finally, lower water absorption resistance, etc (Azeez et al., 2019; Azeez et al.,, 2018; Government et al., 2019(a-c)). Pre-treated APWF has improved cellulosic fiber than the fiber which is not treated due to minimization of hemicelluloses and other components of the fiber (Homkhiew et al., 2014; Laadila et al., 2017; Obasi, 2015; Onuegbu et al., 2014; Sood & Dwivedi, 2018). Therefore, when the pretreated APWF infuses in polymer matrix, the final products will lead to composite with improved qualities. But if the APWF is not treated the reverse effect is reduction of micro-mechanical properties and destruction of the composite with time (Homkhiew et al., 2014; Laadila et al., 2017; Obasi, 2015; Onuegbu et al., 2014; Government & Okeke, 2024).

Early scholars had researched on woody plants in polymer matrix composites for marketing ventures: date palm (Atuanya et al., 2014; Government et al., 2021(a); Government & Okeke., 2023), flame of the forest pod fiber Government et al., 2019(b)). pine wood (Turku et al., 2018), paulownia wood (Tisserar et al., 2014), groundnut shell (Government et al., 2022), mango seed shell fiber (Government et al., 2019(d), roselle fiber (Azeez et al., 2021), etc. This present works entailed the study the influence of particle size on pretreated APWF/LLDPE composite in order to generate low-cost novel material that can act as substitutes to particle board for furniture in automobile parts. The intended APWF-LLDPE was examined at five particles for three different chemical modifying routs. The pretreated

and non-treated APWF-LLDPE composite were taken for SEM and FTIR for surface micro-structural and functional group analysis

2.0 Material and methods

2.1 Experimental

2.1.1 APWF material selection:

The APWF was subjected to drying on the sun for 14 days at 8 hrs after extraction of the bark fiber. The APWF was manually pulverized with sieve of 100-20 mesh (150-850 µm).

2.1.2 Pretreatment of APWF with alkali

The APWF was pre-treated with NaOH solution of 6 wt.% for 16 hrs at 98% purity level manufactured in India, a product of Pvt. Limited. As the pretreatment was concluded, the APWF was decanted and washed with de-ioninized water, filtered and dried in the sun for 10 hrs.

Chemical modified APWF with acid; The APWF was soaked in 6wt.% NaOH for 16 hrs and 4 vol.% of 98% percentage purity of CH_3COOH (made in England by BDH limited) for 1 hr. After pretreatment, decantation of fiber took placed followed by rinsing the APWF demineralized water and dried by the sun for 10 hrs.

2.1.3 Pretreated APWF mixed with maleated polyethylene

The APWF after pretreated with NaOH and CH_3COOH, then combined appropriately with 5wt.% maleated polyethylene (MAPE) produced in United State of America by Sigma-Aldrich Chemical Corporation at 4,200 g × 10 min^{-1} in 190 °C × 2.16 kg^{-1} and 0.905 g × cm^{-3} for melt flow index and density, respectively.

2.1.4 Formulation of APWF-LLDPE composite:

The APWF for unmodified and treated at 5, 10, 15, 20 and 25 wt. % intermixed by 95, 90, 85, 80 and 75 wt.% of LLDPE made in Indorama Petrochemical Limited, PH, Rivers State with 15 g × 10 min^{-1} melt flow index. The pretreated and untreated APWF were infused in the LDPE by melt blending with aid of injection molding machine (model HUICHON/5SON10/500×1000 no.6241) supplied by PO Yuen (TO'S) Machine FTY limited in Democratic People of Republic, Korea. The untreated and pretreated APWF-LLDPE composites compounded after cooling were examined for FTIR, SEM, mechanical and water absorption resistance analysis, respectively.

2.1.5 Tensile, bending and hardness characteristic of APWF-LLDPE composite

The tests were examined in Department of Civil Engineering, UNN applying universal tensometer produced in Hounsefield, England (BSS1610 model 8889). The standards for these analysis were ASTM D638 (3.2mm x 19mm x 160mm), ASTM D790 (3.2mm x 19mm x 300mm) and ASTM E103 (3.2 mm × 19mm ×19mm) correspond for the tensile, flexural and Brinell's hardness characteristic of the composite, respectively(Atuanya et al., 2014). A bulb of 10mm steel was utilized for hardness of the composite. The composite specimen was placed in the machine for determination properties according ASTM standard for tensile strength, elastic modulus, flexural strength and modulus, and Brinell's hardness, respectively. The evaluation of the tensile strength, tensile modulus, flexural strength, flexural modulus, load-deflection slope, and Brinell's hardness were determined applying the corresponding equations. These corresponded by following: Eq. (1), Eq. (2), Eq.(3), Eq.(4), Eq. (5) and Eq.(6), respectively. These were stated as follows:

$$\sigma_T = \frac{f_m}{A_1} \quad (1)$$

$$E_{M} = \frac{\Delta\sigma}{\Delta\varepsilon} \quad (2)$$

$$\sigma = \frac{3FL}{2bd^2} \quad (3)$$

$$E(bend) = \frac{L^3 m}{4Wb^3} \quad (4)$$

$$m = \frac{\Delta F}{\Delta e} \quad (5)$$

$$BHN = \frac{2f}{\pi D\left[D - \sqrt{D^2 - d^2}\right]} \quad (6)$$

The stated parameters in the equations: σ_T, f_m, A_1, E_M, $\Delta\sigma$, $\Delta\varepsilon$, σ, f, d, l, b , represents the tensile strength, optimum tensile force, cross-sectional area, elastic modulus, difference in stress , strain change, flexural strength, weight at the fracture, thickness, support span length and width, respectively. In addition, the flexural modulus, load-

deflection slope, change on deflected load, change in deflection, Brinell's hardness, diameter of bulb, height of indentation, force at Brinell hardness presented as: E(bend), m, ΔF, Δe, BHN, D, d, f, respectively.

2.1.6 Impact strength determination

The device applied for evaluation of the impact strength is LOS LOSENHAUSENWERK DUSSELDORFER MASCHINENBAU AG. DUSSELLDORF, Germany. Model 17562, supplied in 1963. The specification for the analysis is ASTM D610-02M at sample measurement of 3.2 mm × 19 mm× 80mm. After placing the sample in this equipment, the hammer attached with the instrument smacked the APWF-LLDPE composite sample. The impact energy and other associated variable were recorded. The estimation of the impact strength was determined by Eq.(7).

$$IMS = \frac{E_1}{Z_1} \quad (7)$$

The IMS, E_1 and Z_1 are the impact strength, the impact energy and the sample cross-sectional area, respectively.

2.1.7 Water absorption rate of APWF/LLDPE composite sample

The APWF/LLDPE composite sample was evaluated in ASTM D570 at 3.2mm x 19mm x19mm [29]. At the initial stage, the sample was oven-heated at 50 ^{0}C in 1800 seconds and the weight was measured as P_1. The composite sample was inserted in de-ionized water for 12 weeks, after then, sample was dried and weighed as P_2. The relationship was applied for the calculation of water sorption percentage based on Eq. (8) (Government & Okeke, 2024).

$$W_{\%} = \frac{P_2 - P_1}{P_1} \times \frac{100}{1} \quad (8)$$

The water sorption percentage, initial weight and final weight after water sorption are $W_{\%}$, P_1 and P_2, respectively.

2.1.8 FTIR instrumental analysis

The FTIR instrument used is FTIR spectrometer, model 8400S. A mixture of 1.5 mg powdered APWF-LLDPE composite and 0.5 mg KCl was placed inside the FTIR machine, after 5 seconds, the spectrum of corresponding peaks and wavelengths for different functional groups present in the APWF-LLDPE composite is giving out from the machine as output.

2.1.9 SEM surface micro-structure analysis

The scanning electron microscope (SEM) device employed had the model PHENOM ProX with a voltage of 15 KV. The lab sample of APWF-LLDPE of 0.5 gm was infused in a platinum die and inserted in the SEM device. The SEM pictured which indicated micro-structure arrangement of the component of the composite at numerous magnifications was displayed as final image in the system attached with equipment.

3.0 Results and Discussions

Figure 1(a) represents the impact of APWF particle size on the ultimate tensile strength of APWF-LLDPE composite for the unmodified (UNT), chemically influenced by NaOH (NST), NaOH /CH_3COOH(AAT) and NaOH /CH_3COOH/MAPE, respectively. As cited on Fig. 2(a), the tensile strength of APWF-LLDPE composite exhibits a total reduction in particle size of APWF in LLDPE matrix from 150,180, 250, 425 to 850 µm for UNT, NST, AAT and MPT, respectively. For a specific size of APWF at 150 µm, as the fiber content is added in LLDPE matrix from 5 to 25 %, the ultimate tensile of APWF-LLDPE composite declined from 22.91 to 21.03, 25.29 to 24.2, 24.87 to 23.99, 26.3 to 24.93 MPa for UNT, NST, AAT and MPT, respectively. This is due to fragile interphase bonding between APWF and LLDPE matrix during fiber infusion at a fix particle size. Also, at 180 and 250 µm APWF particle, the tensile of APWF-LLDPE composite reduces from 21.61 to 18.77, 24.43 to 22.52, 24.12 to 22.81, 25.4 to 24.19 MPa; and 23.97 to 22.75, 25.18 to 23.74, 24.65 to 22.33, 26.13 to 24.37 MPa, for UNT, NST, AAT and MPT, respectively. In continuation, similar reduction in the tensile strength of APWF-LLDPE composite was experienced from 425 to 850 µm for UNT, NST, AAT and MPT, respectively. The utmost tensile strength of 26.3 MPa was at minimum particle of APWF at 150 µm which is obtained at 5 wt.% APWF of MPT. This observable reason is the phenomenon of lower particle size sufficiently intermixed with the fiber and polymer matrix supplements by chemical modifier couple with a bonding resin which influences the tensile strength of the

manufactured composite. Previous research results had deliberated elsewhere (Patpen et al, 2015; Government, 2021(a); Kandar & Akil, 2016; Government et al., 2022; Homkhiew et al., 2014; Government et al, 2019(a-d); Peng et al., 2015; Rostamiyan et al., 2015).

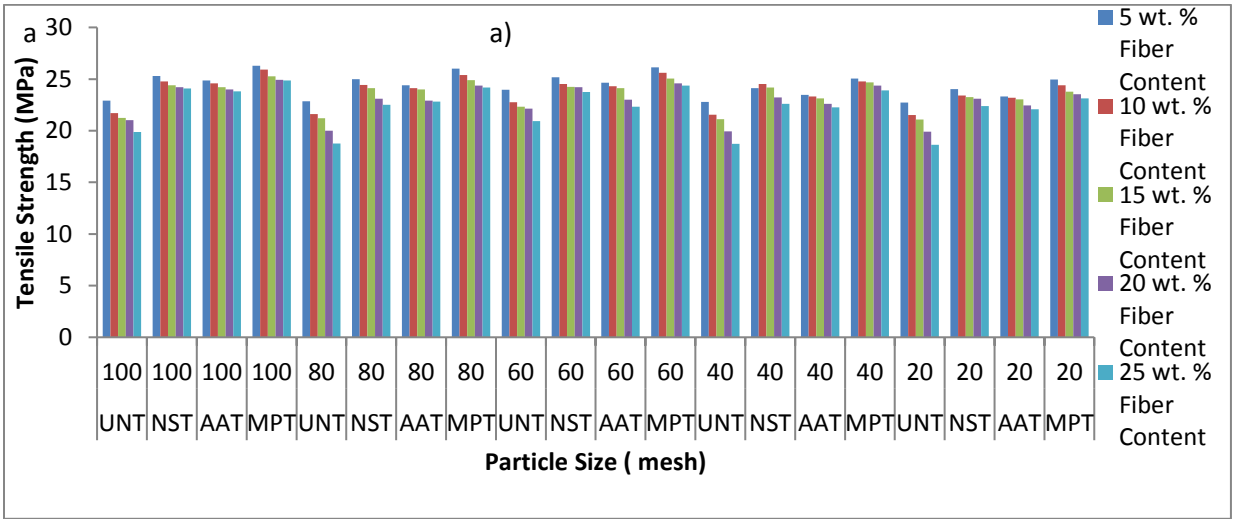


Figure 1(a) The impact of APWF particle size on the ultimate tensile strength of APWF-LLDPE composite for the unmodified (UNT), chemically influenced by NaOH (NST), NaOH /CH_3COOH(AAT) and NaOH /CH_3COOH/MAPE, respectively

The young's modulus of APWF-LLDPE composite diminished when APWF particle size is increased. At 150 µm when the fiber content is added from 5 to 25 wt.% for UNT, NST, AAT and MPT in the LLDPE, the elastic modulus of APWF-LLDPE composite indicates a rise from 0.653 to 0.753, 0.721 to 0.827, 0.689 to 0.817,0.783 to 0.871 GPa , respectively. This is due addition of APWF in the LLDPE curtails the ductility of polymer which causes voids emanation in the APWF-LLDPE composite that leads to increase in stiffiness activated by chemical influence. In the same case, at constant particle of 180 and 250 µm, the elastic modulus of APWF-LLDPE composite continuously declined with arithmetically increment is noticed during the inclusion of fiber content variation. These occurred from 0.645 to 0.748, 0.707 to 0.808, 0.667 to 0.796, 0.765 to 0.853 GPa; and 0.679 to 0.784, 0.713 to 0.816, 0.673 to 0.804, 0.77 to 0.86 GPa, for the unmodified and chemically APWF, respectively.

Moreover, further addition of a higher APWF particle from 425 and 850 µm in the LLDPE matrix, the elastic modulus of APWF-LLDPE composite entirely minimizes. Notwithstanding, the apex young's modulus of APWF-LLDPE composite clustered at 0.871 GPa for MPT which match up with the minimum size employed in the study, this improvement in the modulus of elasticity is due to lower particle size tends to reduces the ductility of the APWF-LLDPE composite which improves the stiffeness as a result of generation of voids at APWF addition in the LLDPE matrix compliment by pretreatment. These voids inhibit mobility which in turns leads to improvement in elastic modulus of APWF-LLDPE composite. Earlier write up had discussed similar situation (Patpen et al, 2015; Government, 2021(a); Kandar & Akil, 2016; Government et al., 2022; Homkhiew et al., 2014; Government et al, 2019(a-d); Peng et al., 2015; Rostamiyan et al., 2015; Government & Okeke, 2023; Government & Okeke, 2024).

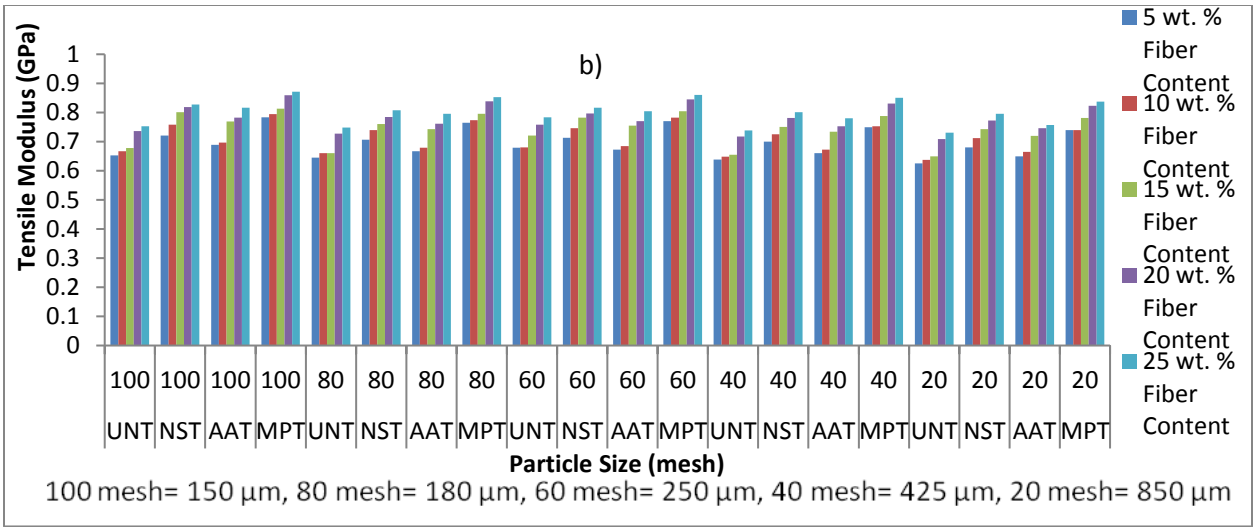


Figure 1(b) displays the influence of APWF size range on the elastic modulus of APWF-LLDPE composite.

The addition of APWF particle from 5 to 25 wt.% in LLDPE at 150 µm for UNT, NST, AAT and MPT improves flexural strength of APWF-LLDPE composite from 40.69 to 43.14, 52.21 to 55.35, 48.81 to 51.97, 60.52 to 63.11 MPa, respectively. Relatively at 180 and 250 µm, the flexural strength of APWF-LLDPE composite reduces as the APWF particle size advances from 40.5 to 43, 47.13 to 50.09, 43.6 to 46.81, 54.38 to 56.92 MPa; and 42.61 to 44.03, 49.21 to 52.18, 45.72 to 48.99, 56.49 to 59.04 MPa, for UNT, NST, AAT and MPT, respectively. In the other hand, the flexural strength of APWF-LLDPE composite lessened at additional APWF particle size from 150-850 µm maintaining its optimum at 100 mesh corresponding to 63. 11 MPa. The phenomenon is an attribution of better strength experiences when APWF particle is slotted in LLDPE matrix which further aggravates with minute size and pretreatment bonds by maleated polyethylene. This was explained by later works (Patpen et al, 2015; Government, 2021(a); Kandar & Akil, 2016; Government et al., 2022; Homkhiew et al., 2014; Government et al, 2019(a-d); Peng et al., 2015; Rostamiyan et al., 2015; Government & Okeke, 2023; Government & Okeke, 2024).

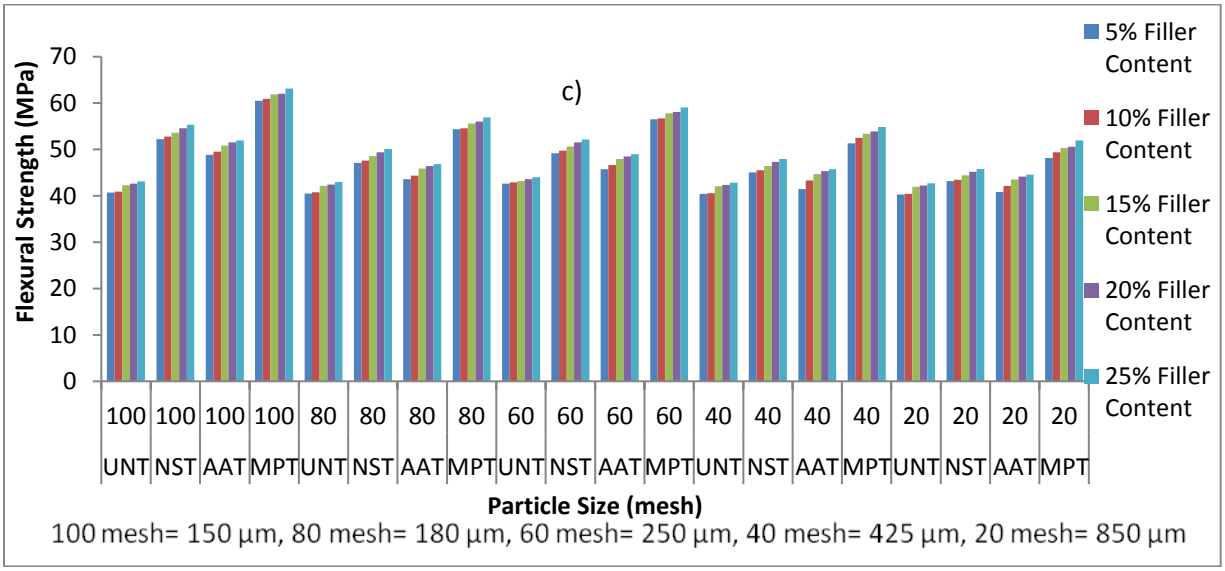


Figure 1(c) describes the influence of APWF size on the flexural strength of APWF-LLDPE composite for UNT, NST, AAT and MPT, respectively.

The impact of APWF size on the flexural modulus of APWF-LLDPE composite for UNT, NST, AAT and MPT is shown in Fig.1 (d). The variation of APWF content in the LLDPE at pre-determined particle size of 150 µm significantly increased the tensile strength of APWF-LLDPE composite from 0.318 to 0.523, 0.502 to 0.691, 0.393

to 0.581, 0.627 to 0.821 GPa for UNT, NST, AAT and MPT, respectively. This is due to adding APWF in the LLDPE, the cellulosic nature of the fiber increases the strength and modulus in the polymer which improves resistance to bending powered by the pretreatment. During the addition of APWF at steady 25 wt.% fiber content, the flexural strength of APWF-LLDPE composite reduces from 0.523 to 0.489, 0.691 to 0.646, 0.581 to 0.547, 0.821 to 0.77 GPa, as APWF size in the LLDPE upgraded from 150-850 µm for UNT, NST, AAT and MPT, respectively.

The furthest flexural modulus of APWF-LLDPE composite is pointed at 0.821 GPa at 150 µm particle size of APWF for MPT. This is due to aspect ratio of 150 µm for APWF is higher than other sizes in LLDPE which homogenizes the polymer with better cellulosic content. This cellulosic content improves the bending stiffness in the polymer and composite during modification by reagents. Familiar trend of result is exhibited at fiber content of 20 wt. %, 15 wt.%, 10 wt%, 5wt.%, respectively. Reporters in field of study encounter related discovery (Patpen et al, 2015; Government, 2021(a); Kandar & Akil, 2016; Government et al., 2022; Homkhiew et al., 2014; Government et al, 2019(a-d); Peng et al., 2015; Rostamiyan et al., 2015; Government & Okeke, 2023; Government & Okeke, 2024).

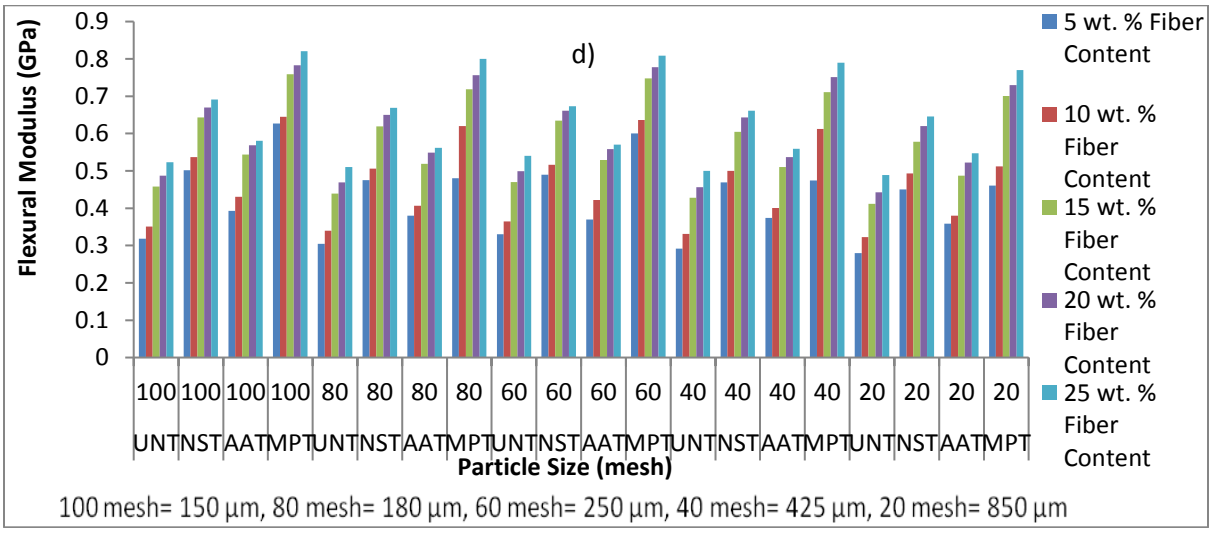


Fig.1 (d): Impact of APWF size on the flexural modulus of APWF-LLDPE composite for UNT, NST, AAT and MPT

The effect of APWF particle size on the hardness of APWF-LLDPE composite for UNT, NST, AAT and MPT is stated in Fig. 1(e). The accumulation of APWF at 150 µm for UNT, NST, AAT and MPT arithmetically into LLDPE matrix improves the resistance to scratch of APWF-LLDPE composite from 162 to 253, 258 to 418, 232 to 402, 278 to 788 Pa, respectively. This situation emanates when APWF particle configures in the LLDPE, the inhibition pressure to abstain indentation and scratches amplify with more of the increment when the APWF particle is added under the control of chemical modification. However, when considering the key factor, particle size variation of APWF-LLDPE composite at 25 wt.% for UNT, NST, AAT and MPT; the Brinell hardness made an absolute decrease from 253 to 213, 418 to 360, 402 to 351, 788 to 720 at 150-850 µm, respectively. The greatest Brinell hardness of APWF-LLDPE composite occurs at 788 Pa at 150 µm for MPT. This observation is due to lower particle of APWF allows more inhibition to indentation with the LLDPE matrix. Also, treatment of APWF further improves the scratching inhibition of the APWF-LLDPE composite. Earlier researcher related outcome (Patpen et al, 2015; Government, 2021(a); Kandar & Akil, 2016; Government et al., 2022; Homkhiew et al., 2014; Government et al, 2019(a-d); Peng et al., 2015; Rostamiyan et al., 2015; Government & Okeke, 2023; Government & Okeke, 2024).

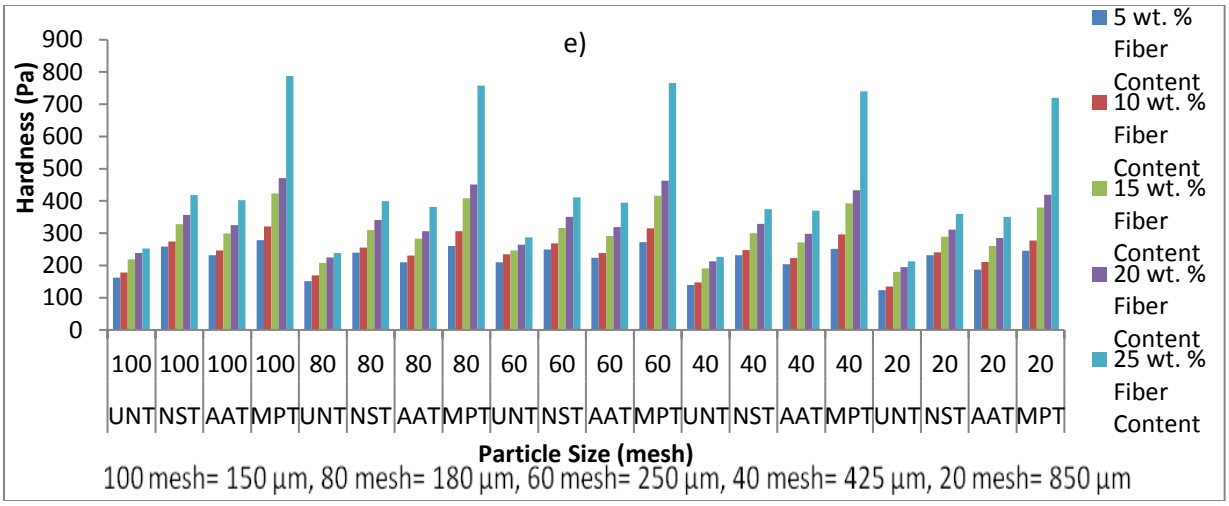


Fig. 1(e): The effect of APWF particle size on the hardness of APWF-LLDPE composite for UNT, NST, AAT and MPT

The dependency of APWF size for UNT, NST, AAT and MPT on the impact strength of APWF-LLDPE composite is represented in Fig. 1(f). The impact strength of APWF-LLDPE composite made a drastic reduction when the fiber content upgrades from 5 to 25 wt.% for a steady particle size of APWF for UNT, NST, AAT and MPT, respectively. This fact is as a result of addition of APWF particle in the LLDPE allows the initiation of cracks propagation and stress on the APWF-LLDPE composite. This stress increases when the APWF content increases which aids the minimization of the impact energy per unit area. Although with chemical influence, the impact strength of APWF-LLDPE composite improves than the untreated one. This is due to activation of APWF with reagents which improves strength and the bending energy of APWF and the LLDPE matrix. In terms of particle size as an influence of APWF, the impact strength of APWF-LLDPE composite depreciated from 59.56 to 59.1, 82.5 to 65.76, 71.12 to 61.06, 90.35 to 66.79 KJ/m^2 with the amplification of particle size from 150-850 µm for UNT, NST, AAT and MPT at 25 wt.%, respectively. Moreover, the pinnacle impact strength of APWF-LLDPE composite is set at 90.35 KJ/m^2 at 150 µm for MPT. This is due to minuscule size of APWF particle tends to improve the union between the APWF and LLDPE interface which has more energy to initialize cracking of the APWF-LLDPE composite. This further improves with the influence of anhydride radical which gives high resistance of the APWF-LLDPE composite to begin cracking. These study concords with previous research (Patpen et al, 2015; Government, 2021(a); Kandar & Akil, 2016; Government et al., 2022; Homkhiew et al., 2014; Government et al, 2019(a-d); Peng et al., 2015; Rostamiyan et al., 2015; Government & Okeke, 2023; Government & Okeke, 2024).

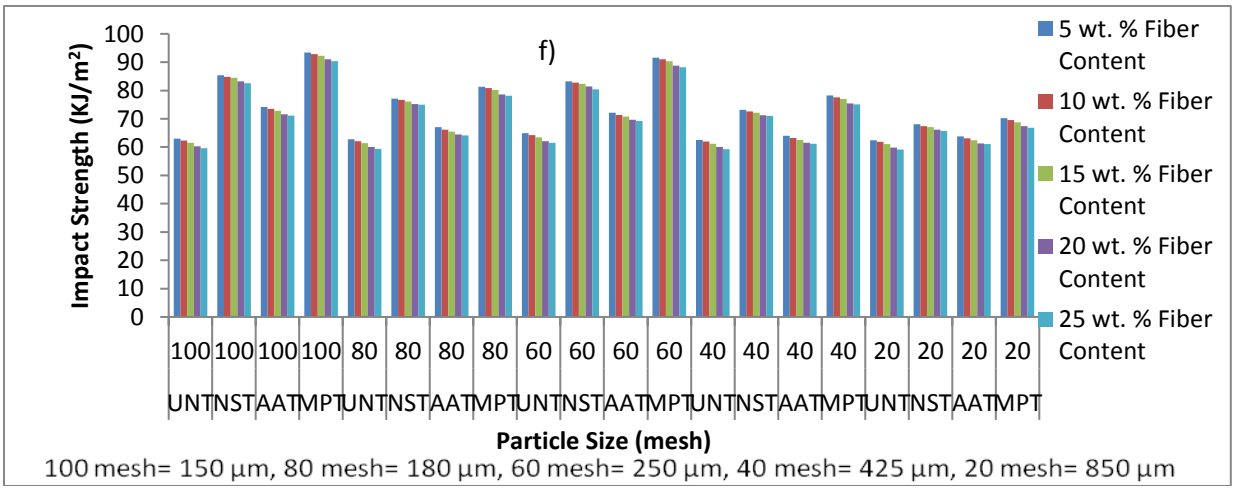


Fig. 1(f): The dependency of APWF size for UNT, NST, AAT and MPT on the impact strength of APWF-LLDPE composite

Figure 1. (g) presents the significant of APWF size on the water absorption of APWF-LLDPE composite. The water absorption resistance of APWF-LLDPE composite reduces when the APWF content amplifies at a particular size for UNT, NST, AAT and MPT, respectively. This is due to more pore spaces is created in APWF-LLDPE composite during addition of APWF content in the LLDPE matrix. This results to the minimization of water absorption resistance of APWF-LLDPE composite. Though, the influence of hydroxyl, acetic and anhydride groups in the pre-treated APWF in the LLDPE matrix also significantly improves water absorption resistance of APWF composite. Finally, the water absorption resistance of APWF-LLDPE composite diminishes from 4.63 to 4.82, 3.89 to 4.28, 4.37 to 4.28,3.49 to 3.94% when the APWF particle is swelled from 150-850 µm at fixed APWF content of 25wt.% for UNT, NST, AAT and MPT, respectively.

Therefore, the water absorption resistance of APWF-LLDPE composite is addressed at 3.49 % at 100 mesh APWF particle for MPT, respectively. This phenomenon occurs due to micro-size of APWF particle adheres to LLDPE matrix after mixing. This merges the APWF-LLDPE composite produce which leads to the amplification of the water resistance of APWF-LLDPE composite. Pretreated APWF-LLDPE composite of APWF by MPT helps to close more of the voids in the LLDPE matrix due to additional bonding of APWF by maleated group in the LLDPE matrix which enhances the sorption resistance of the manufactured composite. Many authors had deliberated on related results (Patpen et al, 2015; Government, 2021(a); Kandar & Akil, 2016; Government et al., 2022; Homkhiew et al., 2014; Government et al, 2019(a-d); Peng et al., 2015; Rostamiyan et al., 2015; Government & Okeke, 2023; Government & Okeke, 2024).

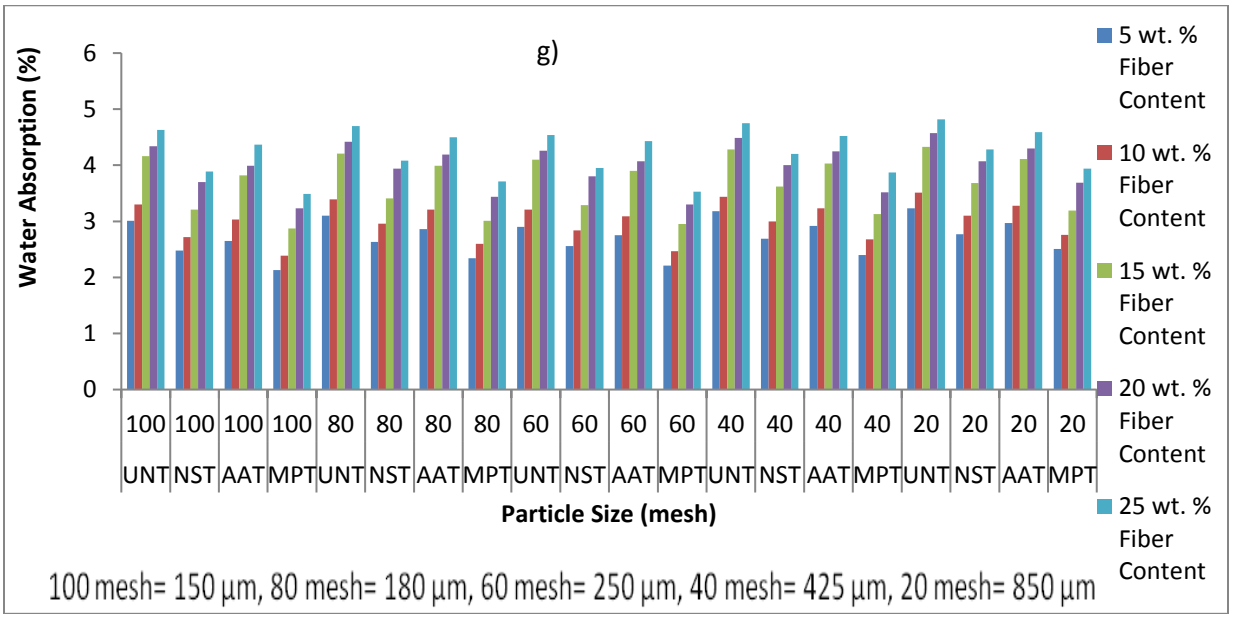
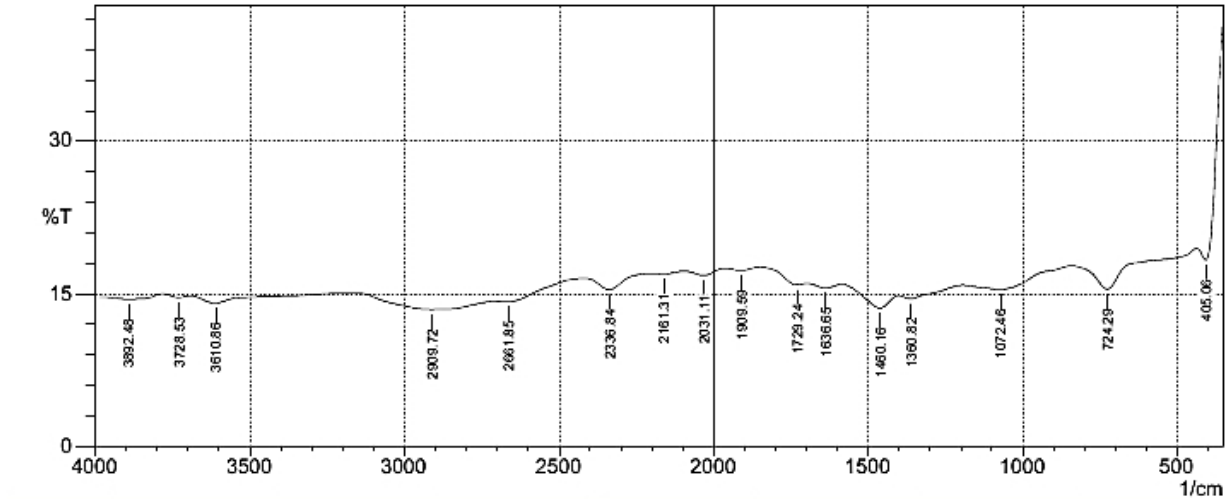


Figure 1. (g) Significant of APWF size on the water absorption of APWF-LLDPE composite.

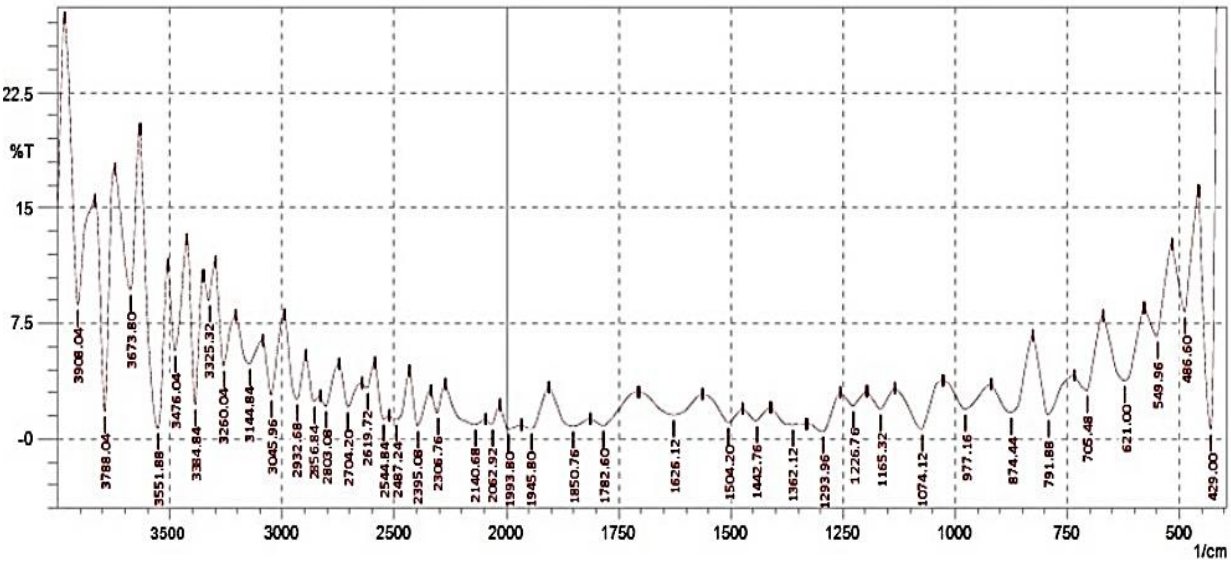
Figure 1: Variation of particle size on the a) tensile strength b) Elastic modulus c) flexural strength d) flexural modulus e) Brinell hardness f) impact strength g) water absorption of HDPE/AWF composite. The spectra in Figure 2 show the FTIR of APWF-LLDPE composite for UNT, NST, AAT and MPT, respectively. The peaks represented in the spectra of APWF-LLDPE composite for UNT, NST, AAT and MPT are captured in Fig.2(a), Fig.2(b), Fig.2(c) and Fig.2(d) as shown, respectively. The wave length at 3738.17-3381.1 cm^{-1}, 2985.48 to 2607.88 cm^{-1}, 2428.68 to 2154.56 cm^{-1}, 2062.92 to 2028.22 cm^{-1}, 1850.76 to 1817.00 cm^{-1} collides with essential radicals in the APWF and APWF-LLDPE composite, respectively. These include radicals in OH^{-} (phenon and alcohol), COOH (carboxyli acid), POOH (phosphorus acid of esters). After treatment, there are changes in peaks position of UNT, NST, AAT and MPT for Fig.2(a), Fig.2(b), Fig.2(c) and Fig.2(d), respectively. These variance in spectria as dispayed in Fig.2(a), Fig.2(b), Fig.2(c) and Fig.2(d), showed that there is highly improvement cellulose drastically minimization of other unwanted constuents after pretreatment of APWF before compounding in LLDPE matrix for the APWF-LLDPE composite. This chemical modification of the fiber optimized the cellulosic component which hardened the bonding potentials and the enhancement of chracteristics of APWF-LLDPE composite for NST, AAT and MPT as can be pictured in Fig.2(b), Fig.2(c) and Fig.2(d), respectively. Similar views were presented by later

scholars in the fields (Patpen et al, 2015; Government, 2021(a); Kandar & Akil, 2016; Government et al., 2022; Homkhiew et al., 2014; Government et al, 2019(a-d); Peng et al., 2015; Rostamiyan et al., 2015; Government & Okeke, 2023; Government & Okeke, 2024).

a)



b)



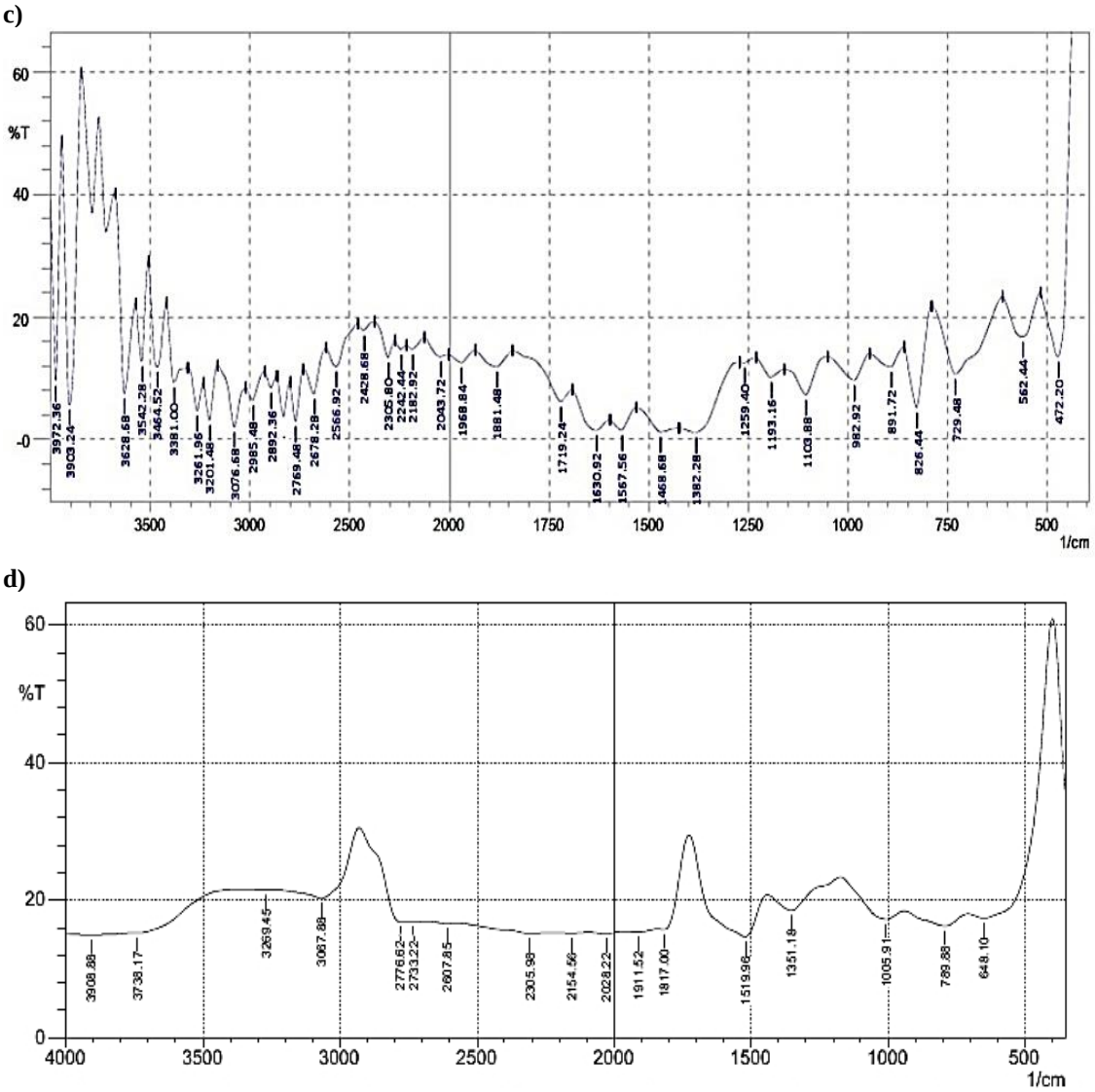


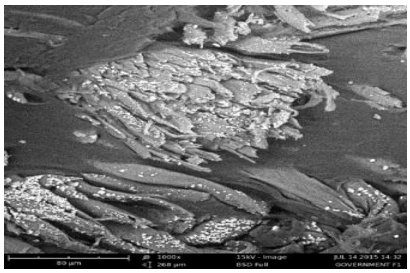
Figure 2: FTIR graph of APWF-LLDPE composite for a) UNT b) NST c) AAT d) MPT at 150 µm at 25 wt.%.

The SEM micrograph of APWF-LLDPE composite for UNT, NST, AAT and MPT is pointed out in Fig. 3(a-d), respectively. As slatted in Figure 3(a), the SEM graph of APWF-LLDPE composite for UNT indicates numerous particles of APWF on the micrograph showing fragile adhesion in the LLDPE matrix. Minute fraction of the APWF-LLDPE composite of UNT displayed union of APWF and LLDPE, while other side of SEM picture established weak union between APWF and LLDPE matrix. This imperfection in the interface of APWF and LLDPE matrix abruptly declines the strength of the composite. The composite strength in the APWF-LLDPE composite for NST as pointed out in Fig. 3(b). The APWF particle reasonable disappeared on the SEM diagram when compared head-to-head with Fig. 3(a). When viewed in Figure 2(a), more of the fractional of SEM monograph showed higher adhesion of APWF and LLDPE matrix.

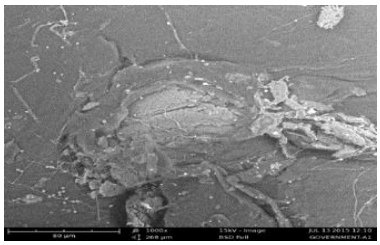
Also, small numbers of cracks were found on the SEM graph which is a sign of inappropriate joining of APWF and LLDPE matrix. This is a substantive basis for the strength of Fig. 3(b) to be greater than Figure 3(a). The SEM monograph of APWF-LLDPE composite for AAT is shown in Fig.3(c). it was noticed few traces of bumps and cracks of unreinforced APWF and LLDPE on the SEM surfaces. Notwithstanding, challenges occurred as a result of particle of APWF not properly dispersed in the LLDPE by lower P^h of acetic acid. This makes the mechanical properties of Fig.3 (b) superior to Fig.3(c). The micro-structural arrangement of APWF-LLDPE composite for MPT is captured in Fig.3(d). The APWF particle and LLDPE matrix indicated greater intermixing in the interface of

APWF-LLDPE with lowest APWF particle found on the SEM. When compared with Fig. 3(c), Fig. 3(b) and Fig. 3(a), the degree of conjunction of APWF and LLDPE matrix in Fig. 3(d) was maximum. This inference was concluded due to MPT contained anhydride group which is by the aid of pretreatment with maleated polyethylene. This trend had been reported by earlier works (Patpen et al, 2015; Government, 2021(a); Kandar & Akil, 2016; Government et al., 2022; Homkhiew et al., 2014; Government et al, 2019(a-d); Peng et al., 2015; Rostamiyan et al., 2015; Government & Okeke, 2023; Government & Okeke, 2024).

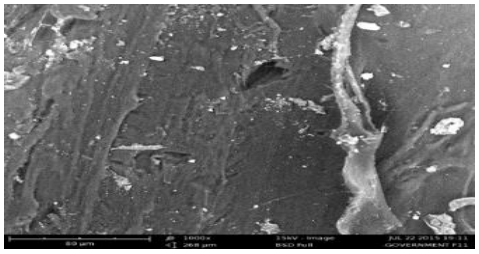
a)



b)



c)



d)

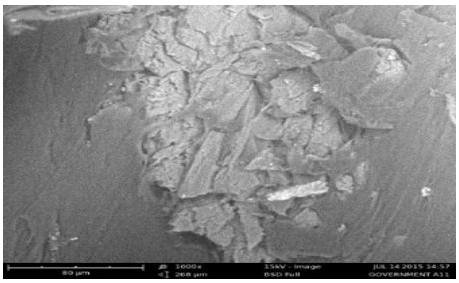


Figure 3: SEM micro-structural picture of APWF-LLDPE composite for {a) UNT (b) NST (c) AAT (d) MPT at 150 µm at 25 wt.%.

4.0. Conclusion

The significant for examination of particle size at steady APWF content was vital factor on properties of APWF-LLDPE Composite blended with different chemically modification stages have been studied. The sizes and content of cheap APWF, preliminary treatment, LLDPE matrix were essential in evaluating the characteristics and sorption résistance of APWF-LLDPE composite. The optimum results were reflected by FTIR and SEM investigation. The minimum particle and the combination of chemical modified APWF with NaOH/CH_3COOH/MAPE infused in LLDPE matrix yielded the better mechanical and absorption resistive capacity of APWF-LLDPE composite. From this outcome derived from this work, the APWF has a prospect with other existing biomass whose potentials can fully be exploited for commercialization of polymer-fiber composite production.

5.0 Recommendation

The APWF-LLDPE composite with the best pre-treatment blending is recommended as a component for furniture in the interior parts of a car panel after the passage seat.

References

Aimi,N. N., Anuar, H., Manshor, M. R., Nazri, W. B. W., & Sapuan, S. M. 2014. Optimizing the parameters in durian skin fiber reinforced polypropylene composites by response surface methodology. Industrial Crops and Products, 54, 291–295. https://doi.org/10.1016/j.indcrop.2014.01.016

Atuanya, C. U., Government, M. R., Nwobi-Okoye, C. C., & Onukwuli, O. D. 2014. Predicting the mechanical properties of date palm wood fibre-recycled low density polyethylene composite using artificial neural network. International Journal of Mechanical and Materials Engineering, 9(1), 1–20. https://doi.org/10.1186/s40712-014-0007-6

Azeez, T. O. 2019. Thermoplastic recycling: properties, modifications, and applications. in polymer recycling (pp. 1–19). Rijeka, Croatia: InTech Open. https://doi.org/http://dx.doi.org/10.5772/intechopen.81614

Azeez, T. O., Government, R. M., Eze, I. O., & Iwuji, S. C. 2021. Modifications and Physicomechanical Behaviors of Roselle Fiber-HDPE Biocomposites for Biomedical Uses. Roselle, 89–102. https://doi.org/10.1016/b978-0-323-85213-5.00013-5

Azeez, T. O., Onukwuli, O. D., Walter, P. E., & Menkiti, M. C. 2018. Influence of chemical surface modifications on mechanical properties of combretum dolichopetalum fiber-high density polyethylene (HDPE) composites. Pakistan Journal of Scientific and Industrial Research Series A: Physical Sciences, 61A(1), 28–34.

Catto, A. L, & Santana, R. M. C. 2018. Influence of coupling agent in polyolefinic composites from post-consumer waste with Eucalyptus Grandis flour. Journal of Materials Science and Engineering B, 3(10), 641–652. https://doi.org/10.17265/2161-6221/2013.10.003

Dungani, R., Karina, M., Subyakto, Sulaeman, A., Hermawan, D., & Hadiyane, A. 2016. Agricultural waste fibers towards sustainability and advanced utilization: A review. Asian Journal of Plant Sciences, 15(1–2), 42–55. https://doi.org/10.3923/ajps.2016.42.55

Fortunati, E., Kenny, J. M., & Torre, L. 2019. Lignocellulosic materials as reinforcements in sustainable packaging systems: Processing, properties, and applications. Biomass, Biopolymer-Based Materials, and Bioenergy: Construction, Biomedical, and Other Industrial Applications, 87–102. https://doi.org/10.1016/B978-0-08-102426-3.00005-9

Government, M. R., Onukwuli, O. D. & Odera, R. S. 2018(b). Optimization of avocado wood flour polymer Composite. Journal of Engineering and Applied Sciences. 13: 99-109

Government, R. M. & Ngabea, S. A. (2023a).. Effect of particle size and filler content on mechanical properties of avocado wood flour-low density polyethylene composite,Journal of Applied Science, Environment and Management, 27 (10), pp. 2303-2313.

Government, R. M. & Ngabea, S. A. (2023b),. Comparative study on the mechanical properties of fillers-recycled low- density polyethylene for printers and car parts production, UNIZIK Journal of Engineering and Applied Sciences, 2(3), pp. 376–387.

Government, R. M. & Okeke, E. T. .(2024). Effect of particle size on the properties of avocado pear wood fiber / low-density polyethylene composite enhanced by pretreatment. Materials Testing, 66(1), pp. 22–35.

Government, R. M. & Okeke, E.T. 2023. Elastic-characteristics of recycled low-density-polyethylene-date palmwood composite by response surface methodology optimization process for structural application. UNIZIK Journal of Engineering and Applied Sciences, 2(2), 358-368.

Government, R. M., Agu, O. S., & Olowokere, J. A. 2019(b). The use of flame of forest pod flour in high density. Acta Technica Corviniensis – Bulletin of Engineering Tome XII | Fascicule 1 [January – March] (8889), 11–14.

Government, R. M., Ani, A. K., & Onukwuli, O. D. 2021(b). Effect of using different chemically modified breadfruit peel fiber in the reinforcement of LDPE composite, 63, 286–292.

Government, R. M., Ani, K. A., Azeez, T. O., & Onukwuli, D. O. 2019(a). Effects of the chemical treatment of avocado pear wood filler on the properties of LDPE composites. Materials Testing, 61(12), 1209–1214.

Government, R. M., Okeke, E. T., Ibrahim, I. A., & Onukwuli, O. D. 2022. Modeling and simulation of tensile properties of r-LDPE/GSF composite using the response surface methododology. Materialpruefung/Materials Testing, 64(3), 446–454 https://doi.org/10.1515/mt-2021-2109.

Government, R. M., Okeke, E. T.,Thaddaeus, J., Ani, A. K., & Onukwuli, O. D 2021(a). Optimization of flexural and impact properties of r-LDPE-DPWF composite for printer parts production. Materials Testing, 63(4), 373-376

Government, R., Olowokere, J., Odineze, C., Anidobu, C., Yerima, E., & Nnaemeka, B. 2019 (d). Influence of Soaking Time and Sodium Hydroxide Concentration on the Chemical Composition of Treated Mango Seed Shell Flour for Composite Application. Journal of Applied Sciences and Environmental Management, 23(1), 21-28. https://doi.org/10.4314/jasem.v23i1.3

Government, R.M., Omukwuli, O.D. & Azeez, T. O. 2019 (c) . Optimization and characterization of the properties of treated avocado wood flour-linear low density polyethylene composites. Alexandria Engineering Journal, 58(3), 891–899. https://doi.org/10.1016/j.aej.2019.08.004

Government, R.M., Onukwuli O.D. & Ani A.K. (2018a). Chemically treated avocado wood flour -LLDPE Composite. Usak University Journal of Material Sciences, 6(1–2), pp. 27–40.

Harun, S., & Geok, S. K. 2016. Effect of sodium hydroxide pretreatment on rice straw composition. Indian Journal of Science and Technology, 9(21). 1-9 https://doi.org/10.17485/ijst/2016/v9i21/95245

Homkhiew, C., Ratanawilai, T., & Thongruang, W. 2014. Optimizing the formulation of polypropylene and rubberwood flour composites for moisture resistance by mixture design. Journal of Reinforced Plastics and Composites, 33(9), 810–823. https://doi.org/10.1177/0731684413518362

Kandar, M. I. M., & Akil, H. M. 2016. Application of Design of Experiment (DoE) for Parameters Optimization in Compression Moulding for Flax Reinforced Biocomposites. Procedia Chemistry, 19, 433–440. https://doi.org/10.1016/j.proche.2016.03.035

Laadila, M. A., Hegde, K., Rouissi, T., Brar, S. K., Galvez, R., Sorelli, L., Cheikh, R. B., Paiva, M., Abokitse, K. 2017. Green synthesis of novel biocomposites from treated cellulosic fibers and recycled bio-plastic polylactic acid. Journal of Cleaner Production, 164, 575–586. https://doi.org/10.1016/j.jclepro.2017.06.235

Ng, M. H., Verma, D., Sabu, T., & Goh, K. L. 2019. Characteristics of johorean elaeis guineensis oil palm kernel shells: Elasticity, Thermal stability, and biochemical composition. Biomass, Biopolymer-Based Materials, and Bioenergy: Construction, Biomedical, and other Industrial Applications. Elsevier Ltd. https://doi.org/10.1016/B978-0-08-102426-3.00004-7

Obasi, Henry C. 2015. Peanut Husk Filled Polyethylene Composites: Effects of Filler Content and Compatibilizer on Properties. Journal of Polymers, 2015, 1–9. https://doi.org/10.1155/2015/189289

Onuegbu, G. C., Obasi, C. H., & Onuoha, F. N. 2014. Tensile behaviour of cocoa pod filled polypropylene composites. Asian Journal of Basic and Applied Sciences, 1(2), 1–7. Retrieved from www.multidisciplinaryjournals.com

Orji, B. O., & McDonald, A. G. 2020. Evaluation of the mechanical, thermal and rheological properties of recycled polyolefins rice-hull composites. Materials, 13(3). https://doi.org/10.3390/ma13030667

Peng Chang, B., Md Akil, H., Bt Nasir, R., & Khan, A. 2015. Optimization on wear performance of UHMWPE composites using response surface methodology. Tribology International, 88, 252–262. https://doi.org/10.1016/j.triboint.2015.03.028

Rajak, D. K., Pagar, D. D., Menezes, P. L., & Linul, E. 2019. Fiber-reinforced polymer composites: Manufacturing, properties, and applications. Polymers, 11(10). https://doi.org/10.3390/polym11101667

Rashid, B., Leman, Z., Jawaid, M., Ghazali, M. J., & Ishak, M. R. 2016. The mechanical performance of sugar palm fibres (ijuk) reinforced phenolic composites. International Journal of Precision Engineering and Manufacturing, 17(8), 1001–1008. https://doi.org/10.1007/s12541-016-0122-9

Rostamiyan, Y, Fereidoon, A., Ghalebahman, A. G., Mashhadzadeh, A. H., & Salmankhani, A. 2014(b). Experimental study and optimization of damping properties of epoxy-based nanocomposite : Effect of using nanosilica and high-impact polystyrene by mixture design approach. Journal of Materials&Design. https://doi.org/10.1016/j.matdes.2014.10.022

Rostamiyan, Y., Hamed Mashhadzadeh, A., & SalmanKhani, A. 2014(a). Optimization of mechanical properties of epoxy-based hybrid nanocomposite: Effect of using nano silica and high-impact polystyrene by mixture design approach. Materials and Design, 56, 1068–1077. https://doi.org/10.1016/j.matdes.2013.11.060

Rostamiyan, Yasser, Fereidoon, A., Mashhadzadeh, A. H., Ashtiyani, M. R., & Salmankhani, A. 2015. Using response surface methodology for modeling and optimizing tensile and impact strength properties of fiber orientated quaternary hybrid nano composite. Composites Part B: Engineering, 69, 304–316. https://doi.org/10.1016/j.compositesb.2014.09.031

Sood, M., & Dwivedi, G. 2018. Effect of fiber treatment on flexural properties of natural fiber reinforced composites: A review. Egyptian Journal of Petroleum, 27(4), 775–783. https://doi.org/10.1016/j.ejpe.2017.11.005

Tisserat, B., Reifschneider, L., Grewell, D., & Srinivasan, G. 2014. Effect of particle size, coupling agent and DDGS additions on Paulownia wood polypropylene composites. Journal of Reinforced Plastics and Composites, 33(14), 1279–1293. https://doi.org/10.1177/0731684414521886

Turku, I., Kärki, T., & Puurtinen, A. 2018. Durability of wood plastic composites manufactured from recycled plastic. Heliyon, 4(3), 1–20. https://doi.org/10.1016/j.heliyon.2018.e00559

Zakaria, M. S., Ghazali, C. M. R., Hussin, K., Wahab, M. K. A., Halim, K. A. A., & Yevon, L. 2018. Characteristic and morphology of palm waste filled thermoplastic composites. Solid State Phenomena, 280 SSP, 415–421. https://doi.org/10.4028/www.scientific.net/SSP.280.415